

# RGS-7 Completes a Receptor-Independent Heterotrimeric G Protein Cycle to Asymmetrically Regulate Mitotic Spindle Positioning in *C. elegans*

Heather A. Hess,<sup>1</sup> Jens-Christian Röper,<sup>3</sup>  
Stephan W. Grill,<sup>3,4</sup> and Michael R. Koelle<sup>2,\*</sup>

<sup>1</sup>Department of Genetics

<sup>2</sup>Department of Molecular Biophysics  
and Biochemistry

Yale University

New Haven, Connecticut 06520

<sup>3</sup>Max-Planck-Institute for Cell Biology and Genetics  
D-01307 Dresden

Germany

## Summary

Heterotrimeric G proteins promote microtubule forces that position mitotic spindles during asymmetric cell division in *C. elegans* embryos. While all previously studied G protein functions require activation by seven-transmembrane receptors, this function appears to be receptor independent. We found that mutating a regulator of G protein signaling, RGS-7, resulted in hyperasymmetric spindle movements due to decreased force on one spindle pole. RGS-7 is localized at the cell cortex, and its effects require two redundant  $G_{\alpha_o}$ -related G proteins and their nonreceptor activators RIC-8 and GPR-1/2. Using recombinant proteins, we found that RIC-8 stimulates GTP binding by  $G_{\alpha_o}$  and that the RGS domain of RGS-7 stimulates GTP hydrolysis by  $G_{\alpha_o}$ , demonstrating that  $G_{\alpha_o}$  passes through the GTP bound state during its activity cycle. While GTPase activators typically inactivate G proteins, RGS-7 instead appears to promote G protein function asymmetrically in the cell, perhaps acting as a G protein effector.

## Introduction

Asymmetric cell divisions allow the unequal distribution of cellular components to daughter cells to specify different cell fates during development. Recent studies in *C. elegans* and *Drosophila* have shown that heterotrimeric G proteins position the mitotic spindle during asymmetric cell divisions (Knust, 2001; Gönczy, 2002). During the first mitotic division in *C. elegans*, the spindle is aligned along the anterior-posterior (A-P) axis, and astral microtubules pull on the centrosomes at the two spindle poles. Greater force is exerted on the posterior than on the anterior pole, causing the entire spindle to be displaced posteriorly, thus resulting in an asymmetric cleavage plane that produces daughter cells of unequal size (Grill et al., 2001). Removal by RNAi of two redundant heterotrimeric G proteins related to mammalian  $G_{\alpha_o}$  results in a symmetric first cell division (Gotta and Ahringer, 2001) due to reduction of force on both centrosomes to similar low levels (Colombo et al., 2003). These

results suggest that  $G_{\alpha_o}$  increases microtubule forces and does so to a greater extent at the posterior than the anterior spindle pole.

Heterotrimeric G proteins have principally been studied as signal transducers, and their mechanism of activation and inactivation in this role has been well documented (Hamm, 1998). They are composed of  $\alpha$ ,  $\beta$ , and  $\gamma$  subunits. In the inactive form,  $G_{\alpha}$  is bound to GDP and  $G_{\beta\gamma}$ . Extracellular ligands activate seven-transmembrane receptors to stimulate the  $G_{\alpha}$  subunit to exchange GDP for GTP. The GTP bound  $G_{\alpha}$  dissociates from  $G_{\beta\gamma}$ , and both are active to signal downstream effectors. Signaling by  $G_{\alpha}$ -GTP and  $G_{\beta\gamma}$  continues until  $G_{\alpha}$  hydrolyzes GTP and the heterotrimer reassociates. The duration of signaling by G proteins must be tightly regulated to produce the appropriate cellular responses. The slow intrinsic rate of GTP hydrolysis by  $G_{\alpha}$  can be dramatically accelerated by a class of proteins called regulator of G protein signaling (RGS) proteins (Berman et al., 1996), which contain a 120 amino acid RGS domain responsible for GTPase activation.

The heterotrimeric G proteins that control *C. elegans* spindle movements operate via an activation/inactivation cycle different from the signal transduction G protein cycle outlined above. Two redundant  $G_{\alpha_o}$ -related  $G_{\alpha}$  proteins, GOA-1 and GPA-16, along with the  $G_{\beta}$  subunit GPB-1 and the  $G_{\gamma}$  subunit GPC-2, are required for proper spindle movements in *C. elegans* embryos (Zwaal et al., 1996; Gotta and Ahringer, 2001). Activation of these G proteins is thought to be receptor independent, since (1) it occurs in the one-cell *C. elegans* zygote, which is encased by an impermeable egg shell, so that no source of an extracellular ligand is obvious; and (2) a set of nontransmembrane proteins have been identified that appear to activate the G proteins in lieu of transmembrane receptor(s). Removal of any of these activators results in spindle movement defects similar to those in embryos lacking the  $G_{\alpha}$  proteins. The activators include the 97% identical GPR-1 and GPR-2 proteins, which contain a GPR/GoLoco motif that binds GOA-1 in its GDP bound form (Colombo et al., 2003; Gotta et al., 2003; Srinivasan et al., 2003). The involvement of  $G_{\alpha_o}$  and GPR/GoLoco proteins in mitotic spindle control appears to be evolutionarily conserved, since the GPR/GoLoco motif protein PINS acts with a  $G_{\alpha_{i/o}}$  protein to control asymmetric neuroblast divisions in *Drosophila* (Schaefer et al., 2000, 2001; Yu et al., 2000), the mammalian GPR/GoLoco protein LGN regulates mitotic spindle organization (Du et al., 2001), and the mammalian  $G_{\alpha_o}$  protein is found associated with the mitotic spindle in cultured cells (Wu and Lin, 1994). In *C. elegans*, GPR-1/2 proteins form a complex with the coiled-coil protein LIN-5, which localizes GPR-1/2 to the cell cortex and mitotic spindle (Gotta et al., 2003; Srinivasan et al., 2003). An additional nonreceptor activator that controls *C. elegans* centrosome movements is RIC-8 (Miller and Rand, 2000), whose mammalian ortholog Ric-8A was recently shown to act in vitro as a guanine nucleotide exchange factor for G proteins including  $G_{\alpha_o}$  (Tall et al., 2003).

Fundamental issues regarding the mechanism of asym-

\*Correspondence: michael.koelle@yale.edu

<sup>4</sup>Present address: Department of Physics, University of California, Berkeley, Berkeley, California 94720.

metric spindle positioning remain unresolved. First, all models propose that asymmetric microtubule forces are generated by greater G protein activity at the posterior than at the anterior pole of the zygote, but it remains unclear how such asymmetric G protein activity is generated. Second, alternative models have been proposed in which either a  $G_{\alpha}$ -GDP/GPR complex or  $G_{\alpha}$ -GTP is the active G protein species that promotes microtubule forces, but it remains to be established which of these species are actually generated and active (Colombo et al., 2003; Gotta et al., 2003; Srinivasan et al., 2003). Third, the mechanism by which an active G protein controls microtubule forces is unknown.

We show here that an RGS protein, RGS-7, controls asymmetric movements of the mitotic spindle. RGS-7 affects force on the anterior but not the posterior spindle pole, suggesting that it is a source of asymmetric G protein function. In vitro, RIC-8 promotes GTP binding by  $G_{\alpha_o}$ , while RGS-7 acts as a  $G_{\alpha_o}$  GTPase activator, demonstrating that  $G_{\alpha_o}$  is present in its GTP bound form as part of its receptor-independent activity cycle. While GTPase activators typically inactivate G proteins, RGS-7 apparently promotes G protein function. RGS-7 could serve dual roles as both a  $G_{\alpha_o}$  inactivator and a  $G_{\alpha_o}$  effector so that its net function is to promote microtubule force.

## Results

### Mutants for Each of the *C. elegans* RGS Genes

To determine if RGS proteins are involved in spindle positioning, we generated mutants for each *C. elegans* RGS gene. Mutants for four RGS genes have been previously characterized (Koelle and Horvitz, 1996; Hajdu-Cronin et al., 1999; Dong et al., 2000), and we produced mutants for the remaining nine RGS homologs. We isolated animals with deletion mutations targeted to coding sequences for the RGS domains, to coding sequences upstream of the RGS domain (thus disrupting the reading frame upstream), or to promoter sequences (Figure 1). Because the RGS domain carries out the G protein GTPase function of RGS proteins (Popov et al., 1997), we expect that mutations that prevent production of this domain should be severe loss-of-function or null alleles. With the possible exceptions of our deletions for *rgs-3* and *rgs-8* (see Figure 1), we have generated such mutations for the entire family of 13 RGS genes.

### *rgs-7* Is the Only RGS Gene Required for Embryonic Viability

Two independent *rgs-7* deletions were lethal, while mutations in the other 12 RGS proteins resulted in relatively healthy, fertile animals. Both *rgs-7* mutations were maternal-effect embryonic lethal, i.e., homozygous mutant progeny of heterozygous parents survived to adulthood, but themselves produced only dead progeny. For the *rgs-7(vs92)* mutation, 97% of these progeny died as embryos, while 3% hatched and arrested as L1 larvae ( $n = 101$ ). The dead embryos produced by *rgs-7* mutant homozygotes mostly arrested after gastrulation and prior to morphogenesis, but later-staged embryos were also seen. These results suggest that the *rgs-7* gene product is produced maternally, loaded into oocytes,

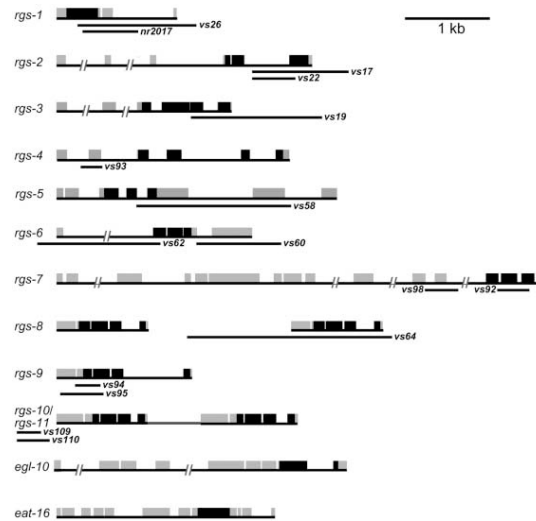


Figure 1. *C. elegans* RGS Genes and Mutations

Coding exons for all 13 RGS genes in *C. elegans* are represented by boxes, with the gene names indicated at left. RGS domain-coding exons are black. Introns longer than 1 kb are indicated with hash marks and are not drawn to scale. Extents of deletions are indicated by lines labeled with allele names under the exon structures. The *egl-10* and *eat-16* genes were not targeted for deletions because many mutations in these genes are already available (Koelle and Horvitz, 1996; Hajdu-Cronin et al., 1999). The *rgs-1* and *rgs-2* deletions have been previously described (Dong et al., 2000). The tandem *rgs-10/11* genes are predicted to produce a dicronic transcript; deletions were targeted to remove the promoter for this transcript. *rgs-3* encodes a single protein with two RGS domains; the *vs19* deletion removes coding sequences encoding the second. *rgs-8* is a duplicated gene, and only one copy was removed by the *vs64* deletion. With the potential exceptions of *rgs-3* and *rgs-8*, the deletions shown appear to be severe loss-of-function or null alleles for each of the 13 RGS genes.

and then has an essential function in embryonic development. The *rgs-7* gene product can also be supplied paternally, since some live progeny were produced by mating wild-type males to otherwise infertile *rgs-7* mutant homozygotes.

We sequenced several *rgs-7* cDNAs and found that *rgs-7* produces two alternative transcripts with different 5' ends that encode proteins (RGS-7a and RGS-7b) with different N termini (Figure 2). The C-terminal region common to the two proteins includes a C2 domain and an RGS domain. One human RGS protein, RGS3, also has an isoform with both C2 and RGS domains (Kehrl et al., 2002). While some C2 domains bind  $Ca^{2+}$ , Sato et al. (2003) found that the RGS-7 C2 domain lacks conserved Asp residues required for  $Ca^{2+}$  binding and that it coprecipitates from homogenates of transfected cells with certain  $G_{\alpha}$  proteins. Thus, this C2 domain may bind directly to G proteins.

Both *rgs-7* deletion mutations remove most or all of the RGS domain coding sequences: *rgs-7(vs92)* deletes RGS domain coding sequences, and *rgs-7(vs98)* causes a shift in the reading frame upstream of the RGS domain (Figure 2). We cannot exclude the possibility that the mutants produce truncated proteins containing the C2 domain that retain some function.

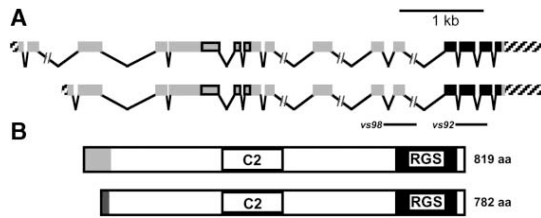


Figure 2. *rgs-7* Transcripts, Mutations, and Proteins

(A) *rgs-7* transcripts and knockout mutations. *rgs-7* produces alternative transcripts, with the *rgs-7a* transcript (upper schematic) using two unique 5' exons that differ from the 5' exon used by the *rgs-7b* transcript (lower schematic). The genomic regions deleted in the *vs98* and *vs92* mutations are indicated as lines below the schematics. Exons are represented by boxes, with the C2 domain coding sequences outlined in black and the RGS domain coding sequences shown in solid black. Introns longer than 1 kb are indicated with hash marks and are not drawn to scale. The 5' and 3' untranslated regions are indicated by hatched boxes. The *vs92* mutation deletes RGS domain coding sequences, while the *vs98* deletion is predicted to disrupt the reading frame upstream of the RGS domain.

(B) Diagrams of the 819 amino acid RGS-7a (upper) and 782 amino acid RGS-7b (lower) protein isoforms. Each contains identical C2 and RGS domains, but the isoforms differ at their N termini: 53 N-terminal amino acids are unique to RGS-7a (light gray box), and 16 N-terminal amino acids are unique to RGS-7b (dark gray box).

### RGS-7 Mutants Show Hyperasymmetric Movement of Mitotic Spindles

The embryonic lethal phenotype of *rgs-7* could result from misregulation of  $G_{\alpha}$  activity in early embryos, leading to defective cell divisions. To test this hypothesis, we examined spindle movements in *rgs-7* mutant embryos. We found defects in the first cell division and have focused our analysis on this stage, as the first observable defects in the mutants are likely to directly reflect the function of RGS-7. Defects in later cell divisions were also seen but might have arisen as indirect consequences of the earlier defects.

Events during the first mitotic cell division in wild-type *C. elegans* embryos are highly reproducible (Schneider and Bowerman, 2003). The nuclei and centrosomes are visible using differential interference contrast microscopy as clearings from which yolk vesicles are excluded (Figure 3A, left panel). As the zygote enters the first mitosis, the pronuclear envelopes break down. During anaphase, the mitotic spindle elongates as the posterior centrosome undergoes oscillations (rocking) perpendicular to the A-P axis (Figure 3A, middle panel). The function of rocking is unknown; it is thought to result from short-lived imbalances in forces on the posterior centrosome (Grill et al., 2001). Ultimately, the spindle is posteriorly displaced to determine an asymmetric cleavage plane that divides the zygote into a larger anterior daughter and a smaller posterior daughter (Figure 3A, right panel).

We analyzed spindle movements by tracing the positions of the two centrosomes at the ends of the spindle using time-lapse video microscopy. These can be plotted as shown for a representative wild-type embryo in Figure 3B. In *rgs-7* mutant embryos, the rocking movements of the posterior centrosome were exaggerated compared to those of the wild-type (compare Figures 3B and 3D). This exaggerated centrosome movement

defect has not been seen previously in any mutant. It is very different from the defect in embryos double-RNAi-treated to remove  $G_{\alpha}$ -1 and GPA-16 (this treatment is hereafter referred to as  $G_{\alpha}$  RNAi), which show no rocking movements (Figures 3E and 3F).

We carried out a quantitative analysis of centrosome movements in wild-type, *rgs-7(vs92)*, *rgs-7(vs98)*, and  $G_{\alpha}$  RNAi embryos (Table 1). Events from fertilization to the onset of the first mitosis were similar in wild-type and *rgs-7* mutant embryos (data not shown). However, *rgs-7(vs92)* embryos show significant increases in the speed and magnitude of posterior centrosome movements during anaphase of the first cell division. This included faster and larger dorsal-ventral (D-V) rocking motions as well as faster and larger posteriorly directed movement as the spindle elongated (Table 1). These movements resulted in the spindle being overdisplaced toward the posterior, resulting in a hyperasymmetric first cleavage (Table 1). Part of the overdisplacement of the spindle midpoint resulted from the anterior spindle pole in *rgs-7* embryos moving toward the posterior, whereas, in the wild-type, this spindle pole moved slightly anteriorly as the spindle elongated. This reverse movement of the anterior centrosome occurred consistently (Table 1) and is illustrated in the plots shown in Figure 3 (compare Figures 3B and 3D). *rgs-7(vs98)* embryos showed defects similar to but weaker than *rgs-7(vs92)* embryos (Table 1). Whereas the *vs92* deletion removes the RGS domain coding sequences from *rgs-7* and may represent a null allele, the *vs98* deletion removes a region 5' to these sequences (Figure 2), and it is possible that use of cryptic splice sites allows production of some transcripts that can encode functional RGS domain-containing protein products.  $G_{\alpha}$  RNAi embryos showed defects that were in several respects opposite those of *rgs-7* mutant embryos (Figure 3, Table 1). All spindle movements in  $G_{\alpha}$  RNAi embryos were reduced, resulting in a symmetrical first cleavage.

*rgs-7* mutant embryos also showed defects after the one-cell stage. At the two-cell stage, five out of ten *rgs-7(vs92)* embryos showed misoriented mitotic spindles in the posterior daughter cell, with the spindle overrotating by more than 20° beyond the alignment along the A-P axis seen in the wild-type. When embryos were not mounted between a coverslip and an agarose pad, even more pronounced spindle misalignments occurred in both cells, leading to grossly misoriented cell divisions (data not shown). It is likely that the accumulation of misoriented cell divisions, which are also seen in RNAi-treated embryos lacking  $G_{\alpha}$  or  $G_{\beta\gamma}$  subunits (Zwaal et al., 1996; Gotta and Ahringer, 2001), leads to the embryonic lethality of *rgs-7* mutants.

In summary, *rgs-7* mutant embryos showed a novel spindle movement defect. The posteriorly directed movements of the spindle seen in the wild-type were exaggerated in *rgs-7* mutant embryos, resulting in hyperasymmetric cell divisions. This contrasts with the reduced spindle movements and reduced asymmetry seen in  $G_{\alpha}$  RNAi embryos.

### *rgs-7* Mutants Have Reduced Force on the Anterior Spindle Pole

Spindle movements during anaphase result from each spindle pole being pulled toward opposite ends of the

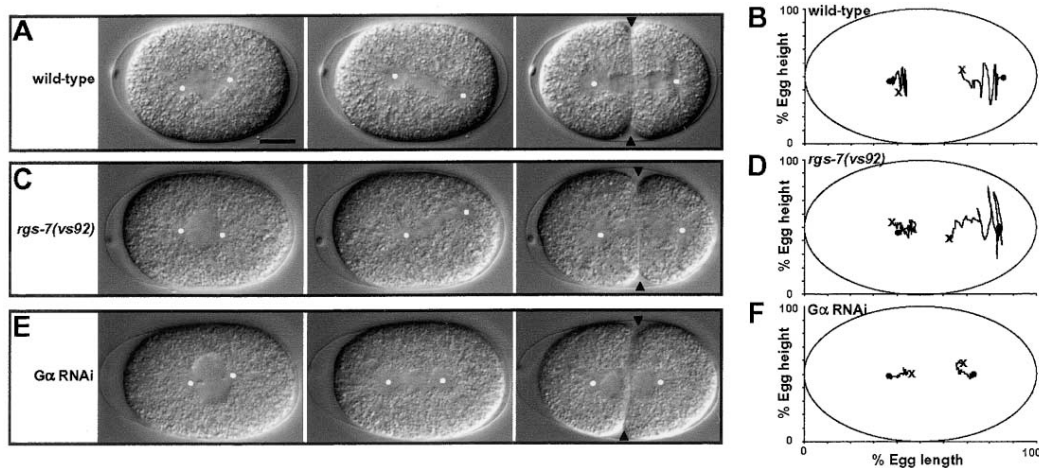


Figure 3. Analysis of Centrosome Movement during the First Cell Division in Wild-Type, *rgs-7*, and  $G\alpha$  RNAi Embryos

(A) Images of a representative one-cell wild-type embryo recorded by time-lapse video microscopy at pronuclear breakdown (left), at anaphase (middle), and at the completion of cytokinesis (right). The complete movies for all embryos shown in Figures 3 and 5 are available in Supplemental Data. Anterior is to the left in this and all subsequent figures. Centrosomes are visualized as clear areas that undergo characteristic changes in size and shape during cell division. White dots indicate the centers of the centrosomes in each image. Arrowheads indicate the position of the cleavage furrow at the end of cytokinesis. Scale bar, 10  $\mu$ m.

(B) Tracing of centrosome movements of the wild-type embryo shown in (A) with the positions of the centrosomes indicated from the onset of mitosis at pronuclear breakdown (positions indicated with x) to the completion of cytokinesis (positions indicated with black circles). The oval is a schematic representation of the egg shell, whose anterior tip (left) is defined as 0% egg length.

(C and D) Images (C) and tracings (D) of a representative *rgs-7(vs92)* embryo undergoing the first mitosis. The rocking movements of the posterior centrosome are greater in magnitude than in the wild-type.

(E and F) Images (E) and tracings (F) of a representative GOA-1/GPA-16 double RNAi ( $G\alpha$  RNAi)-treated embryo. The rocking movements of the posterior centrosome are absent. Thus, RGS-7 and  $G\alpha$  have opposite effects on centrosome movement: *rgs-7* mutants show increased posterior centrosome movement, while  $G\alpha$  RNAi embryos show decreased posterior centrosome movement.

cell. The increased posteriorly directed spindle movements in *rgs-7* mutants could be due to increased pulling on the posterior spindle pole or to decreased pulling on the anterior pole, since either would result in an increased net force toward the posterior. To distinguish between the possibilities, we used a pulsed ultraviolet laser microbeam to sever the spindle midzone at the beginning of spindle elongation. This allows the two spindle poles to independently spring toward their respective ends of the cell. The peak velocities of these

movements can be used as a measure of the pulling forces on each spindle pole (Grill et al., 2001).

We severed spindles in both control and *rgs-7* mutant embryos and compared the resulting spindle pole movements (Figure 4). As seen previously (Grill et al., 2001), control embryos show faster movement of the posterior than the anterior spindle pole after severing. The greater pulling force on the posterior pole demonstrated by this result explains the asymmetric posterior-directed movement of the spindle in wild-type zygotes. In spindle-

Table 1. Quantitation of Centrosome Movements and Spindle Positions in Zygotes

Measurement	Wild-type <sup>a</sup>	<i>rgs-7(vs92)</i> <sup>a</sup>	$G\alpha$ RNAi <sup>a</sup>
Largest half rock <sup>b,c</sup>	19.1 ± 1.4	27.6* ± 1.4	N/A
Maximum D-V speed <sup>d</sup>	0.72 ± 0.04	0.95** ± 0.05	0.11* ± 0.01
Maximum A-P speed <sup>d</sup>	0.20 ± 0.02	0.29* ± 0.02	0.07* ± 0.01
Spindle length ( $\mu$ m) <sup>e</sup>	22.8 ± 0.2	20.7** ± 0.3	13.6* ± 0.6
Position of anterior centrosome <sup>e,f</sup>	38.6 ± 0.6	44.4** ± 0.6	35.6* ± 0.8
Position of posterior centrosome <sup>e,f</sup>	80.6 ± 0.5	83.0* ± 0.4	69.3* ± 0.5
Position of spindle midpoint <sup>e,f</sup>	59.6 ± 0.5	63.7** ± 0.4	52.5* ± 0.6
Position of first cleavage <sup>f,g</sup>	58.6 ± 0.5	60.8* ± 0.7	54.0* ± 0.9

<sup>a</sup>Ten embryos were recorded and measured for each genotype/treatment. Means and 95% confidence intervals are shown. Single asterisks indicate values statistically different from the wild-type with  $p < 0.05$ . Double asterisks indicate measurements whose values in *rgs-7(vs92)* were also statistically different from the wild-type with  $p < 0.05$ .

<sup>b</sup>Half rock is defined as a D-V movement of the posterior centrosome of >4% egg height preceded or followed by another >4% egg height movement in the opposite direction.

<sup>c</sup>Expressed as percentage of egg height.

<sup>d</sup>Speed of the posterior centrosome expressed in  $\mu$ m/s.

<sup>e</sup>Measured at the time of cytokinesis initiation.

<sup>f</sup>Positions are expressed as percentage of egg length with anterior equal to 0%.

<sup>g</sup>Position of the cleavage plane at completion of cytokinesis.

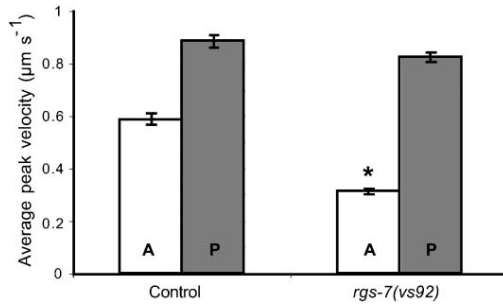


Figure 4. Peak Velocities of Spindle Poles after Spindle Severing in Control and *rgs-7* Mutant Embryos

Bars show the average peak velocities of spindle poles along the anterior-posterior axis ( $n = 26$  for control,  $n = 34$  for *rgs-7* mutant embryos). White and gray bars indicate speeds of anterior and posterior spindle poles, respectively. Error bars are 95% confidence intervals, and the asterisk indicates a significant difference between anterior pole velocities in *rgs-7* versus control embryos ( $p < 0.05$ ). The *unc-20(e112)* marker mutation was used to verify the genotype of the *rgs-7* mutant embryos and was also included in the control embryos for consistency. Mutation of *rgs-7* reduced movement of the anterior pole but had no effect on the posterior pole, suggesting that RGS-7 specifically affects pulling force on the anterior pole.

severed *rgs-7* mutant embryos, there was no significant change in movement of the posterior pole compared to that of spindle-severed control embryos, but the rate of anterior pole movement was decreased by almost 50% (Figure 4). Thus, *rgs-7* zygotes had significantly decreased force pulling on the anterior spindle pole, explaining the exaggerated posteriorly directed movements of their mitotic spindles (Figure 3, Table 1). In contrast, spindle severing has shown that  $G\alpha$  or *gpr-1/2* RNAi reduces force on both spindle poles to similar low levels (Colombo et al., 2003), explaining the reduced and symmetrical spindle movements seen in unsevered  $G\alpha$  and *gpr-1/2* RNAi embryos.

#### The Effects of RGS-7 on Spindle Positioning Require $G\alpha$ and its Nonreceptor Activators GPR-1/2 and RIC-8

A number of G protein signaling components affect spindle movements, but the functional relationships among them remain unclear. Several models for the receptor-independent G protein cycle have been proposed (Colombo et al., 2003; Gotta et al., 2003; Srinivasan et al., 2003). Figure 5A shows a model similar to one of those proposed in Srinivasan et al. (2003), except that we have added RGS-7 acting as a GTPase activator that returns  $G\alpha$ -GTP to its GDP bound form. In this model, a LIN-5/GPR complex acts to dissociate the  $G\alpha$ -GDP/ $G\beta\gamma$  heterotrimer and produce a  $G\alpha$ -GDP/GPR complex and free  $G\beta\gamma$ . Subsequently, RIC-8 uses its hypothetical nucleotide exchange activity to catalyze GTP binding by  $G\alpha$ , causing  $G\alpha$  to dissociate from GPR. Finally, RGS-7 acts as a GTPase activator to return  $G\alpha$  to the GDP bound state, allowing it to reassociate with  $G\beta\gamma$  or GPR. Various models hypothesize that either a  $G\alpha$ -GDP/GPR complex or  $G\alpha$ -GTP could be the species that activates microtubule forces (Colombo et al., 2003; Gotta et al., 2003; Srinivasan et al., 2003).

To examine the relationship between RGS-7 and the

other G protein signaling components that control spindle positioning, we analyzed the effect of removing RGS-7 by mutation in embryos that had been treated with RNAi to remove  $G\alpha$  or its activators. In control embryos with no RNAi treatment (using the same genetic background as for the experimental embryos), removal of RGS-7 increased rocking movements of the posterior centrosome (Figures 5B and 5C). RNAi inactivation of  $G\alpha$  or any of its activators resulted in reduced posterior centrosome movements and the complete absence of posterior centrosome rocking (Figures 5D–5G, upper panels). Mutation of *rgs-7* had no effect in embryos treated with RNAi for  $G\alpha$ , *gpr-1/2*, or *ric-8* (Figures 5D, 5F, and 5G; statistical analysis is presented in Supplemental Table S2 at <http://www.cell.com/cgi/content/full/119/2/209/DC1/>), indicating that the effect of RGS-7 on spindle positioning requires  $G\alpha$  and these nonreceptor activators. Thus, RGS-7 appears to act downstream of  $G\alpha$ , GPR-1/2, and RIC-8 in the regulatory pathway that controls spindle positioning. This is consistent with the model in Figure 5A but does not exclude other models.

The *rgs-7* mutation had somewhat more complex effects in *lin-5* RNAi embryos (Figure 5E, see Supplemental Table S2 on the Cell website). The *rgs-7* mutation had no effect on the reduced movements of the posterior spindle pole seen in *lin-5* RNAi embryos, analogous to the absence of an effect of the *rgs-7* mutation in *gpr-1/2* and *ric-8* RNAi embryos. However, the *rgs-7* mutation did significantly increase the anterior movement of the anterior spindle pole in these embryos, an unexpected effect, since our spindle-severing experiment (Figure 4) showed that the *rgs-7* mutation reduces force on the anterior pole. The meaning of this genetic interaction remains unclear.

#### Subcellular Localization of RGS-7 and RIC-8

We sought to determine the subcellular localization of the RGS-7 and RIC-8 proteins during early embryonic cell divisions. Other components of the model in Figure 5A have previously been localized to the cell cortex ( $G\alpha$ ,  $G\beta$ , LIN-5, GPR-1/2), near the spindle asters/centrosomes ( $G\alpha$ ,  $G\beta$ , LIN-5, GPR-1/2), and the kinetochore microtubules (LIN-5, GPR-1/2) (Gotta and Ahninger, 2001; Colombo et al., 2003; Gotta et al., 2003; Srinivasan et al., 2003; Tsou et al., 2003).

We expressed GFP fused to the N termini of either RGS-7a or RIC-8 in the *C. elegans* germline and examined subcellular localization of these fluorescent proteins during early embryonic cell divisions (Figure 6). For RGS-7, we could not visualize any subcellularly localized fluorescence in the zygote (Figure 6A), but, at the two-cell stage and later, RGS-7::GFP fluorescence was seen at the cell cortex at the junctions between all cells (Figures 6B–6D). For RIC-8::GFP, we again saw faint cortical localization at the junctions between cells (Figures 6E–6H and data not shown). Our failure to detect cortical RGS-7::GFP or RIC-8::GFP fluorescence at the periphery of embryos or the zygote may simply be due to the fact that only a single cell cortex is present, rather than the two opposed cortices present at junctions between cells. RIC-8::GFP showed an additional, dynamic subcellular localization. It was excluded from interphase nuclei and became localized around what appeared to

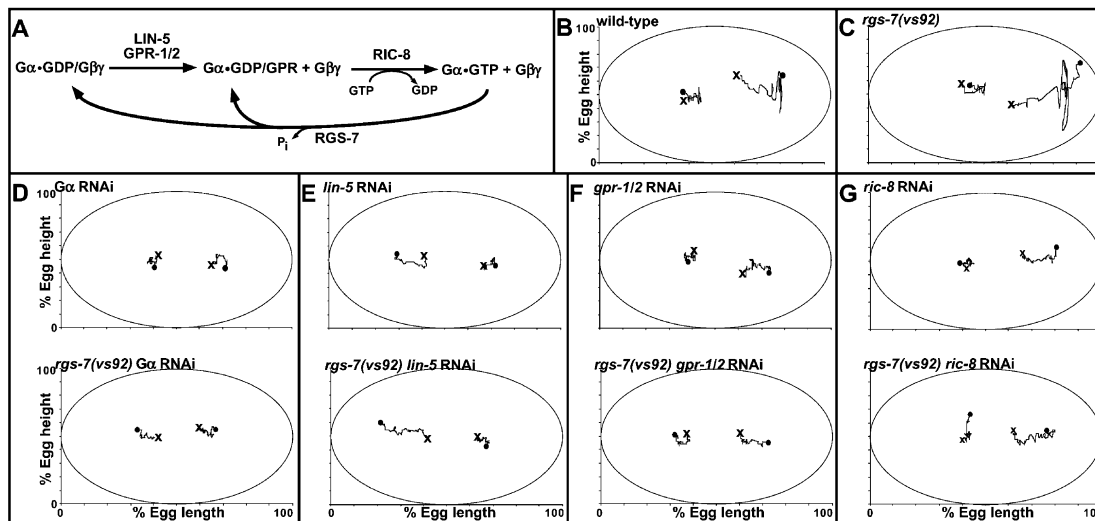


**Figure 5. Analysis of Centrosome Movements in *rgs-7* Mutant Embryos RNAi Treated to Remove  $G\alpha$  or its Nonreceptor Activators**  
**(A)** Model for the receptor-independent G protein cycle. The LIN-5/GPR complex binds  $G\alpha$  and dissociates  $G\beta\gamma$ . RIC-8 subsequently catalyzes nucleotide exchange, dissociating GPR and producing  $G\alpha$ -GTP. RGS-7 acts as a  $G\alpha$  GTPase activator, returning  $G\alpha$  to the GDP bound state that can reassociate with  $G\beta\gamma$  or GPR.  
**(B)** Tracing of centrosome movements of a representative embryo wild-type for all G protein cycle components plotted in the same manner as in Figure 3. This and all other embryos analyzed in this figure carried the *unc-20(e112)* marker mutation, which was used to verify some genotypes and was included in the others for consistency. We found no effect of this marker on centrosome movements.  
**(C)** Tracing of a representative *rgs-7(vs92)* embryo.  
**(D–G)** Tracings of representative embryos in which the indicated G protein cycle components have been inactivated by RNAi (upper panels) or in which these RNAi treatments were combined with the *rgs-7(vs92)* mutation (lower panels). The *rgs-7* mutation increased centrosome movements in the wild-type background but had no effect in  $G\alpha$ , *gpr-1/2*, or *ric-8* RNAi-treated embryos. These results are consistent with the model in (A), which predicts that, when  $G\alpha$  or its activators are absent, preventing production of  $G\alpha$ -GTP, RGS-7 should have no effect.

be kinetochore microtubules at the onset of mitosis, becoming more diffuse during anaphase. This pattern was observed beginning with division of the zygote and repeated in each subsequent cell division (Figures 6E–6H and data not shown). Thus, RGS-7::GFP and RIC-8::GFP were localized to subcellular structures where the other G protein signaling components that control spindle positioning have been observed.

#### RIC-8 and RGS-7 Stimulate GTP Binding and Hydrolysis by GOA-1, Respectively

The model in Figure 5A predicts that RIC-8 stimulates the nucleotide exchange activity of  $G\alpha$  to allow it to bind GTP and that RGS-7 activates GTP hydrolysis by  $G\alpha$  to drive it to the GDP bound form. To test these hypotheses, we expressed and purified recombinant GOA-1, RIC-8, and an RGS domain fragment of RGS-7 (Figure 7A) and used these proteins for *in vitro* activity assays.

We found that purified RIC-8 acted as a nucleotide exchange factor to increase the rate of GTP binding by the  $G\alpha$  protein GOA-1 (Figure 7B). Purified GOA-1 bound to unlabeled GDP was mixed with radiolabeled  $GTP\gamma S$ , a nonhydrolyzable GTP analog, in the presence or absence of purified RIC-8. The rate at which unlabeled GDP was released by GOA-1 and replaced by labeled  $GTP\gamma S$  was measured. GOA-1 showed a low rate of spontaneous nucleotide exchange that was dramatically stimulated by the addition of RIC-8.

We also found that the RGS domain of RGS-7 stimulated the GTPase activity of GOA-1 using a single-turnover GTP hydrolysis assay (Figure 7C). Purified GOA-1

was prebound to  $[\gamma\text{-}^{32}\text{P}]\text{GTP}$  in the absence of  $Mg^{2+}$ , a condition that inhibits GTP hydrolysis. We initiated GTP hydrolysis by adding  $Mg^{2+}$ , with or without the RGS domain of RGS-7, and measured the rate at which  $^{32}\text{P}_i$  was released. The rate of GTP hydrolysis by GOA-1 was dramatically stimulated by the RGS-7 RGS domain. Under the conditions used, RGS-7 stimulated complete hydrolysis of bound GTP within 30 s, whereas GOA-1 in the absence of RGS-7 hydrolyzed only a small fraction of the bound GTP in this time (Figure 7C). Several minutes later (data not shown), GOA-1 eventually hydrolyzed the same amount of GTP in the absence of RGS-7 as in its presence, demonstrating that the effect of RGS-7 is to stimulate the rate and not the extent of GTP hydrolysis by GOA-1.

These results are consistent with the Figure 5A model, in which RIC-8 acts to generate  $G\alpha$ -GTP and RGS-7 uses its GTPase activation activity to return  $G\alpha$  to its GDP bound form.

#### Discussion

##### Different RGS Proteins Regulate $G\alpha_o$ for Its Different Biological Functions

$G\alpha_o$  targets and functions had previously been assigned to four *C. elegans* RGS proteins, and, by knocking out the remaining nine RGS genes, we have identified the function of a fifth, RGS-7. Of the five RGS proteins that now have assigned functions, four act to inhibit the  $G\alpha_o$  protein GOA-1 (Koelle and Horvitz, 1996; Hajdu-Cronin et al., 1999; Dong et al., 2000). In addition to controlling

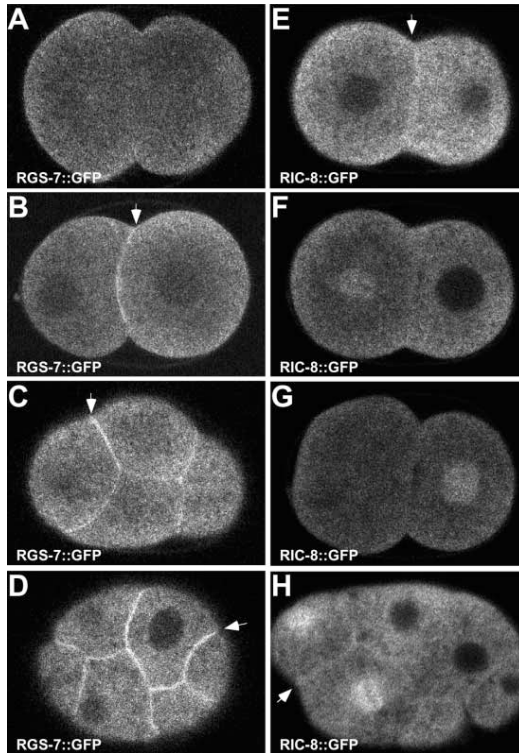


Figure 6. Subcellular Localization of RGS-7::GFP and RIC-8::GFP in Early Embryos

(A–D) Fluorescence of embryos expressing RGS-7::GFP. Arrows indicate fluorescence at a cell junction in each embryo in which such localization is evident. No subcellular localization is evident in the zygote (A), while fluorescence is concentrated at the cell cortex at junctions between cells at the two-cell stage and later (B–D).

(E–H) Fluorescence of embryos expressing RIC-8::GFP. Arrows indicate fluorescence at junctions between cells, which is occasionally evident at the two-cell stage and later (E and H). (E–G) are consecutive photos of a two-cell embryo as the cells progress through the cell cycle. In (E), both cells are in interphase; in (F), the anterior cell (left) has entered mitosis; and, in (G), the anterior cell is in anaphase, while the posterior cell has entered mitosis. Fluorescence is excluded from interphase nuclei, localizes on structures that appear to be kinetochores/microtubules at early mitosis, and then becomes diffuse at anaphase. The same pattern repeats during subsequent cell divisions (H).

embryonic spindle positioning, GOA-1 also acts in adult neurons to transduce signaling by seven-transmembrane neurotransmitter receptors to control behavior of the animal. Genetic studies show that, in adult neurons, the RGS protein EGL-10 sets the baseline level of neurotransmitter signaling through GOA-1, and the redundant RGS-1 and RGS-2 proteins alter GOA-1 signaling under specific circumstances to alter behavior (Dong et al., 2000). Our studies reveal that the multiple RGS proteins acting on the same G $\alpha$  target do so for different biological purposes. This can be partly accounted for by the RGS proteins being expressed in different times and places. RGS-7, for example, functions in early embryogenesis, a time at which the EGL-10 and RGS-1/2 proteins appear not to be expressed (Koelle and Horvitz, 1996; Dong et al., 2000). Another difference between the RGS proteins is that, although they all have RGS domains, they also contain different domains that may

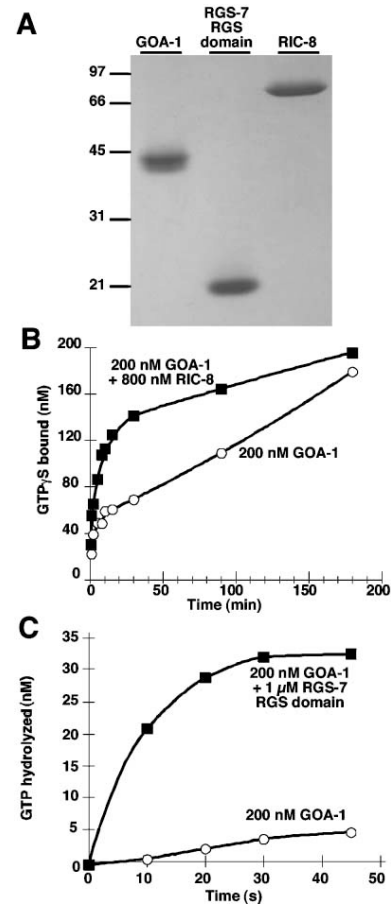


Figure 7. Nucleotide Exchange Activity of RIC-8 and GTPase Activation Activity of the RGS Domain of RGS-7

(A) Coomassie-stained SDS-PAGE gel showing 2  $\mu$ g each of purified recombinant GOA-1, an RGS domain fragment of RGS-7, and RIC-8. The positions of molecular weight markers are indicated, with their sizes in kDa.

(B) Kinetics of GTP $\gamma$ S binding by 200 nM purified GOA-1, with (closed squares) or without (open circles) 800 nM purified RIC-8 protein. Aliquots of the binding reaction were taken at the indicated time points and filtered to absorb protein. The amount of G protein bound [ $^{35}$ S]GTP $\gamma$ S was determined by scintillation counting. Addition of RIC-8 accelerated GTP binding by GOA-1.

(C) Single-turnover GTP hydrolysis assays on GOA-1, with (closed squares) or without (open circles) purified RGS domain from RGS-7. GOA-1 was preloaded with GTP by preincubating with [ $\gamma$ - $^{32}$ P]GTP in the absence of Mg $^{2+}$ . GTP hydrolysis was initiated by adding this GTP-loaded GOA-1 (200 nM) to assay buffer with Mg $^{2+}$ , plus or minus purified RGS domain from RGS-7 (1  $\mu$ M). The release of  $^{32}$ P $_i$  due to GTP hydrolysis was determined over the indicated time course at 4°C. Addition of the RGS-7 RGS domain accelerated GTP hydrolysis by GOA-1.

allow them to act via different mechanisms. For example, the C2 domain found in RGS-7 is absent from EGL-10 and RGS-1/2.

#### RGS-7 Completes a Receptor-Independent G Protein Cycle

Mitotic spindle positioning is controlled by a heterotrimeric G protein cycle that appears to be receptor independent, since the G protein is activated by a set of nontransmembrane proteins. One of the nonreceptor

activators is a complex of the LIN-5 and GPR-1/2 proteins (Gotta et al., 2003; Srinivasan et al., 2003). The GPR proteins contain GPR/GoLoco motifs that have the ability to bind  $G\alpha$ -GDP, removing it from the  $G\alpha$ / $G\beta\gamma$  heterotrimer (Takesono et al., 1999; Ghosh et al., 2003). Thus, all models proposed for the receptor-independent G protein cycle include the existence of a  $G\alpha$ -GDP/GPR complex.

We identified RGS-7 as a protein that controls spindle positioning and found that its RGS domain has GTPase-activating activity on the  $G\alpha$  protein GOA-1. We also found that RIC-8 can catalyze GTP binding by GOA-1 via a nucleotide exchange activity similar to that of its mammalian homolog (Tall et al., 2003). These results strongly favor models like that shown in Figure 5A, in which the receptor-independent G protein cycle is completed by the  $G\alpha$  proteins passing through the GTP bound state. Although our results show that RIC-8 can catalyze nucleotide exchange by GOA-1-GDP, we have yet to test its ability to catalyze exchange on a GOA-1-GDP/GPR complex, the actual RIC-8 substrate predicted in our model.

#### RGS-7 Generates Asymmetric Spindle Force

The characteristic spindle movements in the *C. elegans* zygote result from greater pulling force being applied on the posterior than on the anterior centrosome (Grill et al., 2001). Since force generation depends on the redundant  $G\alpha$  proteins GOA-1 and GPA-16 (Colombo et al., 2003), force asymmetry appears to result from greater activity of the G proteins in the posterior than in the anterior of the embryo. If this is the case, there must be components of the receptor-independent G protein cycle that act differently at the two spindle poles.

Our spindle-severing experiments demonstrate that mutating *rgs-7* affects force on the anterior but not posterior spindle pole. This is the first experimental demonstration that any G protein signaling component has an asymmetric effect on spindle forces. Our results demonstrate that G proteins use a different mechanism to promote force at the two spindle poles. An RGS-7-independent G protein mechanism must act to generate force at the posterior pole, resulting in the greater force observed at that pole.

Previously, both GPR-1/2 and an additional protein, LET-99, have been hypothesized to account for asymmetric G protein activity (Tsou et al., 2002; Colombo et al., 2003; Gotta et al., 2003). GPR-1/2 proteins are candidates to asymmetrically activate  $G\alpha$ , based on their asymmetrical localization at the cortex of zygotes. However, spindle-severing experiments showed that *gpr-1/2* RNAi dramatically reduces force on both spindle poles (Colombo et al., 2003), in contrast to the very asymmetric effects we saw in spindle-severed *rgs-7* mutant embryos. The LET-99 protein affects spindle positioning and also shows an asymmetric distribution in zygotes (Rose and Kempthues, 1998; Tsou et al., 2002, 2003). However, the effects of LET-99 on spindle positioning are complex and have not been analyzed by spindle severing to determine whether LET-99 has an asymmetric effect on spindle forces.

Although RGS-7 asymmetrically affects spindle force, we did not observe an asymmetric distribution of RGS-

7::GFP in zygotes. We cannot exclude the possibility that RGS-7::GFP was asymmetrically localized at the cortex of the zygote but at levels below our threshold of detection. Another possibility is that uniformly distributed RGS-7 is asymmetrically active. Interestingly, LET-99 contains a DEP (dishevelled/EGL-10/pleckstrin) homology domain similar to that found in a number of RGS proteins, including the EGL-10 RGS protein that regulates GOA-1 in adult neurons. In the case of EGL-10, the DEP and RGS domains are both required for function and can be expressed on separate polypeptides to give full activity in vivo (Patikoglou and Koelle, 2002). It is possible that the asymmetrically distributed LET-99 protein interacts with RGS-7 to produce asymmetrical activity of RGS-7.

#### RGS-7 May Be a G Protein Effector that Generates Limited Force

Two fundamental issues remain unresolved regarding the receptor-independent G protein cycle that controls spindle force. First, the identity of the active G protein species remains unclear. In several models, the  $G\alpha$ -GDP/GPR complex is the active species (Gotta et al., 2003; Colombo et al., 2003). Other models hypothesize that  $G\alpha$ -GTP produced by the activity of RIC-8 is the active species (Gotta et al., 2003; Srinivasan et al., 2003). Second, the identity of the effector via which active G protein promotes force on the spindle is unknown.

Our results with RGS-7 present a paradox with respect to the identity of the active G protein species. We found that the RGS domain of RGS-7 acts as a  $G\alpha$  GTPase activator to catalyze removal of  $G\alpha$ -GTP and that a mutation removing the RGS-7 RGS domain resulted in decreased force on the anterior spindle. These results appear to conflict with models in which  $G\alpha$ -GTP is the active species that promotes force. On the other hand, RIC-8 can catalyze production of  $G\alpha$ -GTP, and removal of RIC-8 results in reduced spindle movements (Miller and Rand, 2000; this work) that can most simply be explained by reduced forces on the spindle. These results support models in which  $G\alpha$ -GTP is the active species.

One way to resolve the paradox would be to hypothesize that  $G\alpha$ -GDP/GPR is the active species that promotes force, and the reduced spindle movement defects seen upon removal of RIC-8 are actually the result of increased but symmetrical force. A second way to resolve the paradox would be to hypothesize that RGS-7, in addition to being a  $G\alpha$  GTPase activator, also acts as an effector that allows  $G\alpha$ -GTP to increase microtubule force at the anterior (Supplemental Figure S1). In this scenario,  $G\alpha$ -GTP serves as the active G protein species. Removal of RGS-7, while prolonging the half-life of  $G\alpha$ -GTP, would also prevent  $G\alpha$ -GTP from being able to carry out its function at the anterior, with the net effect of reducing force at the anterior. A precedent for such a scenario is provided by the divergent RGS protein p115RhoGEF, which acts simultaneously as a GTPase activator and an effector. As the RGS domain of p115RhoGEF stimulates the GTPase activity of  $G\alpha_{13}$ , this interaction activates other conserved domains on p115RhoGEF that stimulate the small G protein Rho (Hart et al., 1998). In addition to its RGS domain, RGS-7 contains a conserved C2 domain that could function as an effector to

promote microtubule force, and we note that the C2 domain of synaptotagmin I has been shown to bind tubulin (Honda et al., 2002). Combining the GTPase activation and effector functions in a single polypeptide provides an elegant mechanism to allow G $\alpha$ -GTP to transmit its effects prior to being inactivated. The GTPase activation function of such an effector also ensures that G $\alpha$ -GTP exists and transmits its effects only transiently. Such a mechanism would ensure that only a limited amount of force would be generated on the anterior spindle pole. Perhaps at the posterior pole, G $\alpha$ -GTP transmits force via a non-RGS effector. Lacking a GTPase activation function, this effector would be more persistently activated and thus generate greater force.

#### Experimental Procedures

##### Identification and Knockouts of RGS Genes

A library of frozen mutant worms was screened by PCR for deletions of the *C. elegans* RGS genes identified by Dong et al. (2000). Library construction and screening methods were adapted from Liu et al. (1999) and Edgley et al. (2002) and are described in detail at <http://info.med.yale.edu/mbb/koelle/>. The precise sizes and endpoints of the deleted sequences are available in Supplemental Table S1.

##### cDNA Sequences of *rgs-7* Isoforms

Expressed sequence tags from the database of Dr. Yuji Kohara representing four independent cDNA clones (yk535e4, yk471b4, yk291e11, and yk532h5) identified the *rgs-7a* isoform. We fully sequenced the 2460 bp yk535e4 cDNA clone (GenBank accession number AY569308). The *rgs-7b* isoform was previously described by Sato et al. (2003), who referred to it as C2-RGS. Another potential *rgs-7* isoform is identified by cDNA clone yk1013g3. In this *rgs-7c* isoform, an SL1 leader is *trans*-spliced to the middle of the C2 domain coding sequences. Because it is represented by only a single independent cDNA clone, the existence of the *rgs-7c* transcript is not as well supported as the existence of *rgs-7a* and *rgs-7b*.

##### Maintenance of Lethal *rgs-7* Mutations

*rgs-7* mutants were outcrossed at least four times to the wild-type. Lethal *rgs-7* mutations were maintained heterozygous to the balancer chromosome *unc-1(n496dm) lon-2(e678)*. Homozygous *rgs-7* animals were identified as non-Unc non-Lon progeny, and the embryos from these animals were used for lethal phase determination and for the analysis of centrosome movements presented in Figure 3 and Table 1. For epistasis analysis (Figure 5), *rgs-7(vs92)* mutant embryos were obtained from a different balanced strain: *unc-20(e112) rgs-7(vs92); mnDp33/+*. Unc progeny lack *mnDp33* and show the lethal *rgs-7* mutant phenotype.

##### Analysis of Centrosome Movements in Living Embryos

Animals were dissected in M9 buffer on coverslips, inverted onto agarose pads, and mounted on a Zeiss Axioskop microscope equipped with differential interference contrast optics. Time-lapse movies of embryos were recorded using Openlab software (Improvision) from shortly after fertilization to the end of the first mitotic cell division (a period of ~475 s). Every 2.5 s, images of eight focal planes separated by 1.2  $\mu$ m were recorded. All recordings were at ~23°C. One image from each 2.5 s time point was selected in which the centrosomes were most easily visualized. We manually marked the center of the centrosomal areas in each image, using Openlab software to derive the XY coordinates and precise time point for each mark. These data were used for calculations and statistical analysis.

##### RNA Interference

The coding regions of *goa-1*, *gpa-16*, *gpr-1*, *gpr-2*, *lin-5*, and *ric-8* were amplified by PCR (see Supplemental Experimental Procedures) and used for in vitro RNA synthesis (RiboMAX T7 RNA synthesis kit, Promega). The RNA products were annealed, and dsRNA was

injected into adult hermaphrodites at 0.5–1 mg/ml as described by Fire et al. (1998). G $\alpha$  RNAi embryos analyzed in Figure 3 and Table 1 were produced by coinjection of *goa-1* and *gpa-16* dsRNA into wild-type (N2) animals. For epistasis experiments, the same dsRNAs were injected into both *unc-20(e112)* animals and *unc-20(e112) rgs-7(vs92)* animals. After 24 hr at 20°C, progeny of injected animals were analyzed. For epistasis experiments, three RNAi-treated *unc-20* embryos and five RNAi-treated *unc-20 rgs-7* mutant embryos were recorded and analyzed by time-lapse video microscopy for each RNAi treatment.

##### Spindle Severing

Experiments were performed as described by Grill et al. (2001).

##### Localization of RGS-7::GFP and RIC-8::GFP in Early Embryos

GFP transgenes were generated using the complex array method (Kelly et al., 1997). cDNAs were inserted in pKR2.40 (a gift of G. Seydoux) to express GFP fused to the amino terminus of RGS-7a or RIC-8 using the *pie-1* promoter and 3' UTR. One representative line was selected for each transgene, and embryos were imaged with a Bio-Rad MRC-1024 confocal microscope.

##### Purification of Recombinant Proteins

GOA-1 was purified as described by Dong et al. (2000). Briefly, the protein was expressed in *E. coli* at 19°C with glutathione S-transferase and a tobacco etch virus (TEV) cleavage site at the N terminus. The protein was purified on glutathione agarose, cleaved with TEV protease, and further purified by anion exchange and gel filtration. The RGS domain of RGS-7 was purified in the same manner. RIC-8 was purified analogously, except that an N-terminal His(6) tag was used that was not cleaved from the fusion protein. His(6)-RIC-8 was purified on Ni-NTA agarose and gel filtration columns.

##### Biochemical Assays

Single-turnover GTP hydrolysis assays were as described by Krumin and Gilman (2002). GOA-1 was preloaded with [ $\gamma$ - $^{32}$ P]GTP in the absence of Mg $^{2+}$  and separated from unbound GTP using a Sephadex G25 spin column. GTP hydrolysis was initiated at 4°C by adding 200 nM GOA-1 (about 15% of which was bound to GTP) to an assay mix containing Mg $^{2+}$  and 0 or 1  $\mu$ M RGS-7 RGS domain. Aliquots were withdrawn at various times to stop buffer (5% activated charcoal in 50 mM NaH $_2$ PO $_4$ ). After centrifugation to pellet the charcoal (containing unhydrolyzed GTP), the supernatant was analyzed by scintillation counting to measure  $^{32}$ P $_i$  release. RGS-7 by itself had no detectable GTPase activity (data not shown).

Nucleotide exchange was measured as described by Carty and Iyengar (1994). Purified GOA-1 (200 nM) was assayed at 20°C with or without 1  $\mu$ M purified RIC-8 in 20 mM HEPES (pH 8.0), 100 mM NaCl, 10 mM MgCl $_2$ , and 1 mM DTT containing 10  $\mu$ M [ $^{32}$ S]GTP $\gamma$ S at 10,000 DPM/pmol. Aliquots were withdrawn at various time points and passed through nitrocellulose filters to absorb protein bound GTP $\gamma$ S, and the filters were washed and analyzed by scintillation counting. Purified RIC-8 by itself had no detectable GTP binding activity (data not shown).

##### Acknowledgments

We thank M. Gotta and Y. Kohara for cDNA clones, K. Miller for help with RIC-8 purification, the S. van den Heuvel lab and A. Hyman for advice and discussions, and the NIH and the Leukemia and Lymphoma Society for funding.

Received: April 30, 2004

Revised: September 15, 2004

Accepted: September 16, 2004

Published online: September 23, 2004

##### References

- Berman, D.M., Kozasa, T., and Gilman, A.G. (1996). The GTPase-activating protein RGS4 stabilizes the transition state for nucleotide hydrolysis. *J. Biol. Chem.* 271, 27209–27212.
- Carty, D.J., and Iyengar, R. (1994). Guanosine 5'-O-( $\gamma$ -Thio)triphos-

- phate binding assay for solubilized G proteins. *Methods Enzymol.* 237, 38–44.
- Colombo, K., Grill, S.W., Kimple, R.J., Willard, F.S., Siderovski, D.P., and Gönczy, P. (2003). Translation of polarity cues into asymmetric spindle positioning in *Caenorhabditis elegans* embryos. *Science* 300, 1957–1961.
- Dong, M.Q., Chase, D., Patikoglou, G.A., and Koelle, M.R. (2000). Multiple RGS proteins alter neural G protein signaling to allow *C. elegans* to rapidly change behavior when fed. *Genes Dev.* 14, 2003–2014.
- Du, Q., Stukenberg, P.T., and Macara, I.G. (2001). A mammalian Partner of inscuteable binds NuMA and regulates mitotic spindle organization. *Nat. Cell Biol.* 3, 1069–1075.
- Edgley, M., D'Souza, A., Moulder, G., McKay, S., Shen, B., Gilchrist, E., Moerman, D., and Barstead, R. (2002). Improved detection of small deletions in complex pools of DNA. *Nucleic Acids Res.* 30, e52.
- Fire, A., Xu, S., Montgomery, M.K., Kostas, S.A., Driver, S.E., and Mello, C.C. (1998). Potent and specific genetic interference by double-stranded RNA in *Caenorhabditis elegans*. *Nature* 391, 806–811.
- Ghosh, M., Peterson, Y.K., Lanier, S.M., and Smrcka, A.V. (2003). Receptor- and nucleotide exchange-independent mechanisms for promoting G protein subunit dissociation. *J. Biol. Chem.* 278, 34747–34750.
- Gönczy, P. (2002). Mechanisms of spindle positioning: focus on flies and worms. *Trends Cell Biol.* 12, 332–339.
- Gotta, M., and Ahringer, J. (2001). Distinct roles for  $G_{\alpha}$  and  $G_{\beta\gamma}$  in regulating spindle position and orientation in *Caenorhabditis elegans* embryos. *Nat. Cell Biol.* 3, 297–300.
- Gotta, M., Dong, Y., Peterson, Y.K., Lanier, S.M., and Ahringer, J. (2003). Asymmetrically distributed *C. elegans* homologs of AGS3/PINS control spindle position in the early embryo. *Curr. Biol.* 13, 1029–1037.
- Grill, S.W., Gönczy, P., Stelzer, E.H., and Hyman, A.A. (2001). Polarity controls forces governing asymmetric spindle positioning in the *Caenorhabditis elegans* embryo. *Nature* 409, 630–633.
- Hajdu-Cronin, Y.M., Chen, W.J., Patikoglou, G., Koelle, M.R., and Sternberg, P.W. (1999). Antagonism between  $G_{\alpha}$  and  $G_{\alpha}$  in *Caenorhabditis elegans*: the RGS protein EAT-16 is necessary for  $G_{\alpha}$  signaling and regulates  $G_{\alpha}$  activity. *Genes Dev.* 13, 1780–1793.
- Hamm, H.E. (1998). The many faces of G protein signaling. *J. Biol. Chem.* 273, 669–672.
- Hart, M.J., Jiang, X., Kozasa, T., Roscoe, W., Singer, W.D., Gilman, A.G., Sternweis, P.C., and Bollag, G. (1998). Direct stimulation of the guanine nucleotide exchange activity of p115 RhoGEF by  $G_{\alpha_{13}}$ . *Science* 280, 2112–2114.
- Honda, A., Yamada, M., Saisu, H., Takahashi, H., More, K.J., and Abe, T. (2002). Direct,  $Ca^{2+}$ -dependent interaction between tubulin and synaptotagmin I. *J. Biol. Chem.* 277, 20234–20242.
- Kehrl, J.H., Srikumar, D., Harrison, K., Wilson, G.L., and Shi, C.S. (2002). Additional 5' exons in the RGS3 locus generate multiple mRNA transcripts, one of which accounts for the origin of human PDZ-RGS3. *Genomics* 79, 860–868.
- Kelly, W.G., Xu, S., Montgomery, M.K., and Fire, A. (1997). Distinct requirements for somatic and germline expression of a generally expressed *Caenorhabditis elegans* gene. *Genetics* 146, 227–238.
- Knust, E. (2001). G protein signaling and asymmetric cell division. *Cell* 107, 125–128.
- Koelle, M.R., and Horvitz, H.R. (1996). EGL-10 regulates G protein signaling in the *C. elegans* nervous system and shares a conserved domain with many mammalian proteins. *Cell* 84, 115–125.
- Krumins, A.J., and Gilman, A.G. (2002). Assay of RGS protein activity *in vitro* using purified components. *Methods Enzymol.* 344, 673–685.
- Liu, L.X., Spoerke, J.M., Mulligan, E.L., Chen, J., Reardon, B., Westlund, B., Sun, L., Abel, K., Armstrong, B., Hardiman, G., et al. (1999). High-throughput isolation of *Caenorhabditis elegans* deletion mutants. *Genome Res.* 9, 859–867.
- Miller, K.G., and Rand, J.B. (2000). A role for RIC-8 (Synembryn) and GOA-1 ( $G_{\alpha}$ ) in regulating a subset of centrosome movements during early embryogenesis in *Caenorhabditis elegans*. *Genetics* 156, 1649–1660.
- Patikoglou, G.A., and Koelle, M.R. (2002). An N-terminal region of *Caenorhabditis elegans* RGS proteins EGL-10 and EAT-16 directs inhibition of  $G_{\alpha}$  versus  $G_{\alpha}$  signaling. *J. Biol. Chem.* 277, 47004–47013.
- Popov, S., Yu, K., Kozasa, T., and Wilkie, T.M. (1997). The regulators of G protein signaling (RGS) domains of RGS4, RGS10, and GAIP retain GTPase activating protein activity *in vitro*. *Proc. Natl. Acad. Sci. USA* 94, 7216–7220.
- Rose, L.S., and Kemphues, K. (1998). The *let-99* gene is required for proper spindle orientation during cleavage of the *C. elegans* embryo. *Development* 125, 1337–1346.
- Sato, M., Moroi, K., Nishiyama, M., Zhou, J., Usui, H., Kasuya, Y., Fukuda, M., Kohara, Y., Komuro, I., and Kimura, S. (2003). Characterization of a novel *C. elegans* RGS protein with a C2 domain: evidence for direct association between C2 domain and  $G_{\alpha}$  subunit. *Life Sci.* 73, 917–932.
- Schaefer, M., Shevchenko, A., Shevchenko, A., and Knoblich, J.A. (2000). A protein complex containing Inscuteable and the  $G_{\alpha}$  binding protein Pins orients asymmetric cell divisions in *Drosophila*. *Curr. Biol.* 10, 353–362.
- Schaefer, M., Petronczki, M., Dorner, D., Forte, M., and Knoblich, J.A. (2001). Heterotrimeric G proteins direct two modes of asymmetric cell division in the *Drosophila* nervous system. *Cell* 107, 183–194.
- Schneider, S.Q., and Bowerman, B. (2003). Cell polarity and the cytoskeleton in the *Caenorhabditis elegans* zygote. *Annu. Rev. Genet.* 37, 221–249.
- Srinivasan, D.G., Fisk, R.M., Xu, H., and van den Heuvel, S. (2003). A complex of LIN-5 and GPR proteins regulates G protein signaling and spindle function in *C. elegans*. *Genes Dev.* 17, 1225–1239.
- Takesono, A., Cismowski, M.J., Ribas, C., Bernard, M., Chung, P., Hazard, S., III, Duzic, E., and Lanier, S.M. (1999). Receptor-independent activators of heterotrimeric G-protein signaling pathways. *J. Biol. Chem.* 274, 33202–33205.
- Tall, G., Krumins, A.M., and Gilman, A. (2003). Mammalian Ric-8A (Synembryn) is a heterotrimeric  $G_{\alpha}$  protein guanine nucleotide exchange factor. *J. Cell Biol.* 278, 8356–8362.
- Tsou, M.F., Hayashi, A., DeBella, L.R., McGrath, G., and Rose, L.S. (2002). LET-99 determines spindle position and is asymmetrically enriched in response to PAR polarity cues in *C. elegans* embryos. *Development* 129, 4469–4481.
- Tsou, M.F., Hayashi, A., and Rose, L.S. (2003). LET-99 opposes  $G_{\alpha}$ /GPR signaling to generate asymmetry for spindle positioning in response to PAR and MES-1/SRC-1 signaling. *Development* 130, 5717–5730.
- Wu, H.C., and Lin, C.T. (1994). Association of heterotrimeric GTP binding regulatory protein (Go) with mitosis. *Lab. Invest.* 71, 175–181.
- Yu, F., Morin, X., Cai, Y., Yang, X., and Chia, W. (2000). Analysis of Partner of Inscuteable, a novel player of *Drosophila* asymmetric divisions, reveals two distinct steps in Inscuteable apical localization. *Cell* 100, 399–409.
- Zwaal, R.R., Ahringer, J., van Luenen, H.G., Rushforth, A., Anderson, P., and Plasterk, R.H. (1996). G proteins are required for spatial orientation of early cell cleavages in *C. elegans* embryos. *Cell* 86, 619–629.

#### Accession Numbers

The GenBank accession number for the RGS-7A mRNA sequence reported in this paper is AY569308.